


ORIGINAL ARTICLE

Hypoxia promotes vasculogenic mimicry formation by vascular endothelial growth factor A mediating epithelial-mesenchymal transition in salivary adenoid cystic carcinoma

Hao-fan Wang¹ | Sha-sha Wang¹  | Min Zheng² | Lu-ling Dai¹ | Ke Wang¹ |
Xiao-lei Gao¹ | Ming-xin Cao¹ | Xiang-hua Yu¹ | Xin Pang¹ | Mei Zhang¹ |
Jing-biao Wu¹ | Jia-shun Wu¹ | Xiao Yang¹ | Ya-jie Tang³ | Yu Chen⁴ | Ya-ling Tang⁴ |
Xin-hua Liang¹

¹State Key Laboratory of Oral Diseases, Department of Oral and Maxillofacial Surgery, National Clinical Research Center for Oral Diseases, West China Hospital of Stomatology (Sichuan University), Chengdu Sichuan, China

²Department of Stomatolog, Zhoushan Hospital, Wenzhou Medical University, Zhoushan, China

³Key Laboratory of Fermentation Engineering (Ministry of Education), Hubei Provincial Cooperative Innovation Center of Industrial Fermentation, Hubei Key Laboratory of Industrial Microbiology, Hubei University of Technology, Wuhan, China

⁴State Key Laboratory of Oral Diseases, Department of Oral Pathology, National Clinical Research Center for Oral Diseases, West China Hospital of Stomatology (Sichuan University), Chengdu Sichuan, China

Correspondence

Ya-ling Tang, State Key Laboratory of Oral Diseases, West China Hospital of Stomatology (Sichuan University), Chengdu Sichuan, China.

Email: tangyaling@scu.edu.cn and

Xin-hua Liang, Department of Oral and Maxillofacial Surgery, West China College of Stomatology (Sichuan University), Chengdu Sichuan, China.

Email: lxh88866@scu.edu.cn

Funding information

National Natural Science Foundation of China, Grant/Award Number: 81672672, 81772891, 81572650 and 81502357; Fundamental Research Funds for the Central Universities; Natural Science Foundation of Zhejiang Province, Grant/Award Number: Q142114001; Zhoushan Science and Technology Bureau Project, Grant/Award Number: 2014C3106; Sichuan Province Science and Technology Bureau Project, Grant/Award Number: 2017JY0024

Abstract

Objectives: To investigate the role of hypoxia in vasculogenic mimicry (VM) of salivary adenoid cystic carcinoma (SACC) and the underlying mechanism involved.

Materials and methods: Firstly, wound healing, transwell invasion, immunofluorescence and tube formation assays were performed to measure the effect of hypoxia on migration, invasion, EMT and VM of SACC cells, respectively. Then, immunofluorescence and RT-PCR were used to detect the effect of hypoxia on VE-cadherin and VEGFA expression. And pro-vasculogenic mimicry effect of VEGFA was investigated by confocal laser scanning microscopy and Western blot. Moreover, the levels of E-cadherin, N-cadherin, Vimentin, CD44 and ALDH1 were determined by Western blot and immunofluorescence in SACC cells treated by exogenous VEGFA or bevacizumab. Finally, CD31/ PAS staining was performed to observe VM and immunohistochemistry was used to determine the levels of VEGFA and HIF-1 α in 95 SACC patients. The relationships between VM and clinicopathological variables, VEGFA or HIF-1 α level were analysed.

Results: Hypoxia promoted cell migration, invasion, EMT and VM formation, and enhanced VE-cadherin and VEGFA expression in SACC cells. Further, exogenous VEGFA markedly increased the levels of N-cadherin, Vimentin, CD44 and ALDH1, and

Wang, Wang and Zheng contributed equally to this work.

This is an open access article under the terms of the Creative Commons Attribution License, which permits use, distribution and reproduction in any medium, provided the original work is properly cited.

© 2019 The Authors. *Cell Proliferation* Published by John Wiley & Sons Ltd

inhibited the expression of E-cadherin, while the VEGFA inhibitor reversed these changes. In addition, VM channels existed in 25 of 95 SACC samples, and there was a strong positive correlation between VM and clinic stage, distant metastases, VEGFA and HIF-1 α expression.

Conclusions: VEGFA played an important role in hypoxia-induced VM through regulating EMT and stemness, which may eventually fuel the migration and invasion of SACC.

1 | INTRODUCTION

Salivary adenoid cystic carcinoma (SACC) is one of the most common malignant cancers of the salivary glands accounting for approximately 30% of all salivary malignant tumours.¹⁻³ As an epithelial malignant tumour, SACC is characterized by early haematogenous dissemination, high incidence of lung metastasis and perineural spread.^{4,5} The growth of SACC is quite slow and the 5-year survival rates are 70%-90%. However, the 5-year survival rates of patients with distant metastasis are only 20%.⁶ Hence, it is necessary to address the underlying molecular mechanisms regulating metastatic dissemination of SACC.

Vasculogenic mimicry (VM), proposed by Maniotis in 1999, was defined as a type of vessel-like structures lined with tumour cells without endothelial cells.⁷ VM had been found to evaluate in various aggressive cancers, including colorectal cancer,⁸ breast cancer,⁹ melanoma,¹⁰ and head and neck squamous cell carcinoma,¹¹ suggesting that it was a novel hallmark of cancer. As newly defined mechanism to supply oxygen and nutrition to tumour cells, the high expression of VM was also viewed as a risk factor for poor prognosis, low survival, and invasion and metastasis in cancer patients.¹² Recently, increasing evidence has showed that hypoxic microenvironment not only accelerated tumour invasion and metastasis, but also led to VM formation^{13,14} and the expression of hypoxia-inducible factor-1 α (HIF-1 α) was associated with VM in many cancers types, including breast cancer,¹⁵ ovarian cancer¹⁶ and colorectal cancer.¹⁷ Moreover, Ahluwalia et al reported that HIF-1 by hypoxia condition adjusted vascular endothelial growth factor A (VEGFA) expression at the transcriptional level. VEGFA was a downstream target of HIF-1, and angiogenesis produced by hypoxia was usually VEGFA-dependent.¹⁸ And hypoxia induced EMT by regulating VEGFA. However, it is still not clear whether VEGFA is involved in the hypoxia microenvironment mediating VM formation.^{19,20}

In the previous study, our group has observed that CD133⁺ stem-like SACC cells contributed to the migration and invasion of SACC through inducing VM formation.²¹ Here, we used a three-dimensional culture model to detect VM formation in SACC cell lines under hypoxia condition and found that hypoxia contributed to the migration and invasion, epithelial-mesenchymal transition (EMT) and VM formation of SACC cells. Overexpression of VEGFA boosted VM

formation, the expression of VE-cadherin, N-cadherin, CD44 and ALDH1 in SACC cells. In addition, the presence of VM was positive association with the levels of VEGFA and HIF-1 in SACC samples. These indicated that hypoxia may serve as an inducer of VM in SACC by targeting VEGFA-mediated EMT.

2 | MATERIALS AND METHODS

2.1 | Ethics statement

All studies carried out on human specimens were approved by the Institutional Ethics Committee of the West China Medical Center, Sichuan University, China (No. WCHSIRB-ST-2012-075). Every patient signed separate informed consent forms for sampling and molecular analysis.

2.2 | Cell culture

The high metastatic potential cell line, SACC-LM, and poor metastatic potential cell line (SACC-83) were obtained from the State Key Laboratory of Stomatology, Sichuan University. All cell lines were maintained in high glucose DMEM (HyClone, USA) (10% foetal calf serum, HyClone), 100 U/mL penicillin (Beyotime Biotechnology, China) and 0.1 mg/mL streptomycin (Beyotime Biotechnology) and incubated at 37°C at 5% CO₂. Change the frequency of culture solution according to the growth rate and medium colour. Cells were passaged when cells covered 80%-90% of the bottom.

2.3 | Cell treatments

Cells were cultured in medium contained exogenous VEGFA (100 ng/mL, R&D, USA) and bevacizumab (inhibitor of VEGFA, 125 μ g/mL, Selleck, USA), respectively.

2.4 | Migration assays

Cells (2×10^5 /well) were seeded in 6-well plates. When grow to 80%-90% confluence, cells were scraped with 200 μ L sterile micropipette tip to create a wound. The gap was photographed by inverted culture microscope (magnification, $\times 40$). After 24 hours, the gap filling was photographed.

2.5 | Invasion assay

Cell invasion was performed by BD BioCoat™ Matrigel™ Invasion Chamber (BD Biosciences, USA) according to the manufacturer's protocol. Briefly, cells (5×10^4 cells) were plated on the top chamber in serum-free DMEM and 10% FBS in DMEM in the bottom chamber. Cells were counted at a 100× magnification in standard microscopy 24 hours later.

2.6 | Immunofluorescence

Cells were washed with 1× PBS for 3 minutes, fixed with 4% paraformaldehyde for 20 minutes and washed for three times with 1× PBS for 3 minutes. Then, cells were treated with 0.5% Triton X-100 for 20 minutes at room temperature (this step was omitted when the antigen is expressed on the cell membrane) and washed with 1× PBS. Blocking was performed by normal goat serum for 30 minutes, followed by addition of primary antibody: rabbit anti-E-cadherin (1:400 dilutions, ProteinTech, China), anti-N-cadherin (1:300 dilutions, ProteinTech), rabbit anti-Vimentin (1:200 dilutions, ProteinTech), rabbit anti-VE-cadherin (1:200 dilutions, ProteinTech) and rabbit anti-VEGFA (1:200 dilutions, ProteinTech) to incubate overnight at 4°C, and then washed for three times with PBS. Add 1:200 fluorescent secondary antibody: goat anti-Rabbit Alexa 488 (1:200 dilutions, ZSGB-BIO, China), goat anti-Rabbit Alexa 594 (1:200 dilutions, ZSGB-BIO) and incubated at 37°C in dark for 2 hours. Add DAPI, incubated in dark for 5 minutes, washed with PBS for three times, and observed under a fluorescence microscope.

2.7 | Vasculogenic mimicry assays

Wells of 24-well plate were coated with Matrigel basement membrane matrix (BD). It was allowed to polymerase at room temperature for 1 hour and 37°C for 30 minutes. Cells were resuspended and seeded into a well at a density of 1×10^5 /mL, and then, the experimental group was incubated in a hypoxic incubator at 37°C, 94% N₂, 5% CO₂ and 1% O₂, while the control group was cultured in a normoxic incubator at 37°C, 5% CO₂ and 21% O₂. Cell morphology and formation of cord-like structures were observed using fluorescence inverted microscope (Olympus, Japan). Forty-eight hours later, the length of tubes per field was quantified by counting in five randomly chosen 100× scopes. After 48 hours, the expression of VE-cadherin and VEGFA was observed by immunofluorescence microscopy.

2.8 | Scanning electron microscopy (SEM)

Cells cultured on a coverslip were rinsed with ice-cold 1× PBS (pH 7.2) and fixed with 2% glutaraldehyde for 3 hours at 4°C. After washing with 1× PBS, the cells were fixed with 1% OsO₄ for 2 hours and dehydrated in ethanol. The samples were then critical-point dried and sputter-coated with gold. Samples were examined, and images were acquired using a HITACHI S-520 scanning electron microscope.

2.9 | Confocal laser scanning microscopy (CLSM)

The cells were fixed in 4% paraformaldehyde (PFA) in 1× PBS at room temperature for 20 minutes. The cells were first pre-treated and then blocked in 1× PBS with 0.5% Triton X-100 and 5% BSA for 1 hour. Next, the samples were incubated with anti-VEGFA (1:200 dilutions, ProteinTech) overnight at 4°C, followed by incubation with secondary antibodies goat anti-Rabbit Alexa 488 (1:200 dilutions, ZSGB-BIO). The samples were then analysed with a laser confocal microscope (OLYMPUS IX83, UltraVIEW VoX) with a 640 nm pulse. The images were collected with the Volivity software containing Acquisition, Quantitation and Visualization modules.

2.10 | Flow cytometry (FCM)

The pre-treated cells were harvested and washed twice with FCM buffer (PBS with 5% FBS and 0.1% NaN₃). Cells were resuspended in PBS and incubated with PE-anti-human CD144 (BD Biosciences) for 30 minutes at 4°C.

2.11 | Tumoursphere formation assay

For the tumoursphere formation assay, SACC-LM cells were seeded at a density of 800 cells/ mL of tumoursphere formation medium in ultra-low attachment 12-well plates for 12 days. The tumourspheres formed (spherical, non-adherent cell-masses >90 μm in diameter) were photographed and counted under inverted phase contrast microscope.

2.12 | Western-blot

The isolated cells were lysed in lysis buffer. The protein concentration was then determined. Equal amounts of protein were analysed by SDS-PAGE, followed by electrophoretic transfer to PVDF membranes (Millipore Corp., Billerica, MA, USA). The membrane was blocked for 1 hour with 5 mL blocking buffer (5% skim milk in TBST) and incubated overnight at 4°C with 5% skim milk diluted primary antibody: Rabbit anti-Human VE-cadherin antibody (1:500 dilutions, ProteinTech); Rabbit anti-Human VEGFA antibody (1:500 dilutions, ProteinTech); and Rabbit anti-Human GAPDH antibody (1:500 dilutions, ProteinTech). The next day, the membranes were washed three times with TBST and incubated with 2% skim milk diluted secondary antibody for 2 hour. After washing, the immunoreactive protein bands were visualized using the BIO-RAD gel imaging system. GAPDH was used as an internal control.

2.13 | Real-Time PCR (RT-PCR)

Total RNA was extracted from cells using Trizol (Invitrogen, USA). Then, we synthesized cDNA using a reverse transcription kit (TaKaRa, China) following the manufacturer's instructions. Primer sequences used for PCR were as follows: VE-cadherin: F: ATGAGATCGTGGTGGGAAGCG R: TGTGTACTIONTGGTCTG

GGTGA; VEGFA: F: CAGGCTGCTGTAACGATGAA R: TTTCTTGGCCTTTCGTTTTT; Vimentin: F: ACC AAG ACA CTA TTG GCC GCC T R: CCC TCA GGT TCA GGG AGG AAA AGT; E-Cadherin: F: ATTGCTCACATTTCCCAACTC R: GTCACCTCAGCCATCCT; N-cadherin: F: TGCGGTACAGTGTAACTGGG R: GAAACCGGG CTATCTGCTCG; Twist1: F: TGTCGCGTCCCCTAGC R: TGTCCTTTCTCCTTCTCTGG; Snail: F: GACTACCGCTGCTCCATTCCA R: TCCTCTTACACTAATGGGGCTTT; Slug1: F: AGATGC ATATTCGGACCCAC R: CCTCATGTTTGTGCAGGAGA; VEGFR1: F: ACCTCCGTGCATGTGTATGA R: TGGTGCATGGTTCTGTTGTT; VEGFR2: R: CCGTCAAGGAAAGACTACG R: AGATGCTCCAAG GTCAGGAA; GAPDH: F: TGGCCAAGGTCATCCATGAC R: TGTCATACCAGGAAATGAGCTTG.

2.14 | Immunohistochemical (IHC) and histochemical double-staining methods

Specimens of surgical tumour tissues from SACC patients were fixed with 4% formalin, paraffin embedded and sectioned (4 μ m). The tissue sections were then deparaffinized and dehydrated followed by incubation in 3% hydrogen peroxide for 10 minutes. Slides were stained with primary antibodies at 4°C overnight after blocking with appropriate serum. Corresponding secondary antibodies were used for 1h at room temperature. Targeted molecules were detected

following DAB staining for immunohistochemistry. Tissues were sectioned for CD31 immunohistochemical staining, followed by PAS staining. Slides were finally counterstained with haematoxylin. Two independent investigators blinded to sample identify the anti-VEGFA antibody (1:200 dilutions, ProteinTech) and anti-CD31 antibody (1:100 dilutions, ProteinTech) primary antibody, respectively. PBS was used as the primary antibody for the negative controls.

2.15 | Statistical analysis

The data were recorded as mean \pm SD (standard deviation) and evaluated by SPSS 21.0. Differences between groups were analysed by Student's *t* test or chi-squared test. *P* < 0.05 was considered to indicate a statistically significant result.

3 | RESULTS

3.1 | Hypoxia contributed to migration and invasion, and EMT of SACC cells

To investigate the role of hypoxia in SACC, we applied wound healing and transwell invasion assays to observe migration and invasive abilities under hypoxia. As shown in Figure 1A,B, hypoxia dramatically increased the migratory and invasive behaviours of SACC-83 and

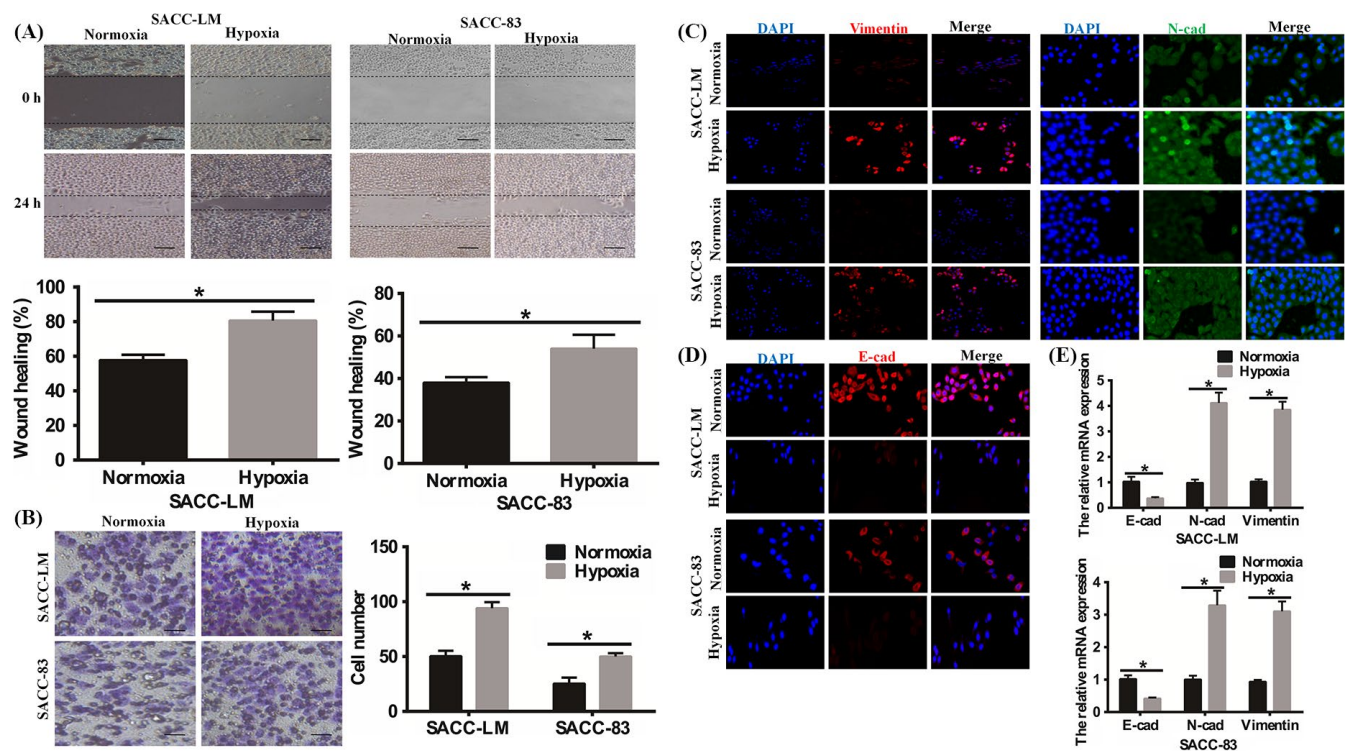


FIGURE 1 Changes in the capacity of invasion and metastasis of the SACC cells. A, Wound healing assays (magnification, $\times 40$; bars, 200 μ m) revealed that hypoxia promoted cells migration of SACC-LM and SACC-83. The results were statistically significant ($*P < 0.05$). B, Number of invasion cells was assessed in the invasion assay (magnification, $\times 100$; bars, 100 μ m). Results showed that hypoxia enhanced SACC cells invasion ($*P < 0.05$). C, The immunofluorescence staining showed that hypoxia up-regulated the expression of N-cadherin and Vimentin (magnification, $\times 100$). D, The immunofluorescence staining showed that hypoxia down-regulated the level of E-cadherin (magnification, $\times 100$; bars, 100 μ m). E, The RT-PCR showed the changes of E-cadherin, N-cadherin and Vimentin in mRNA level

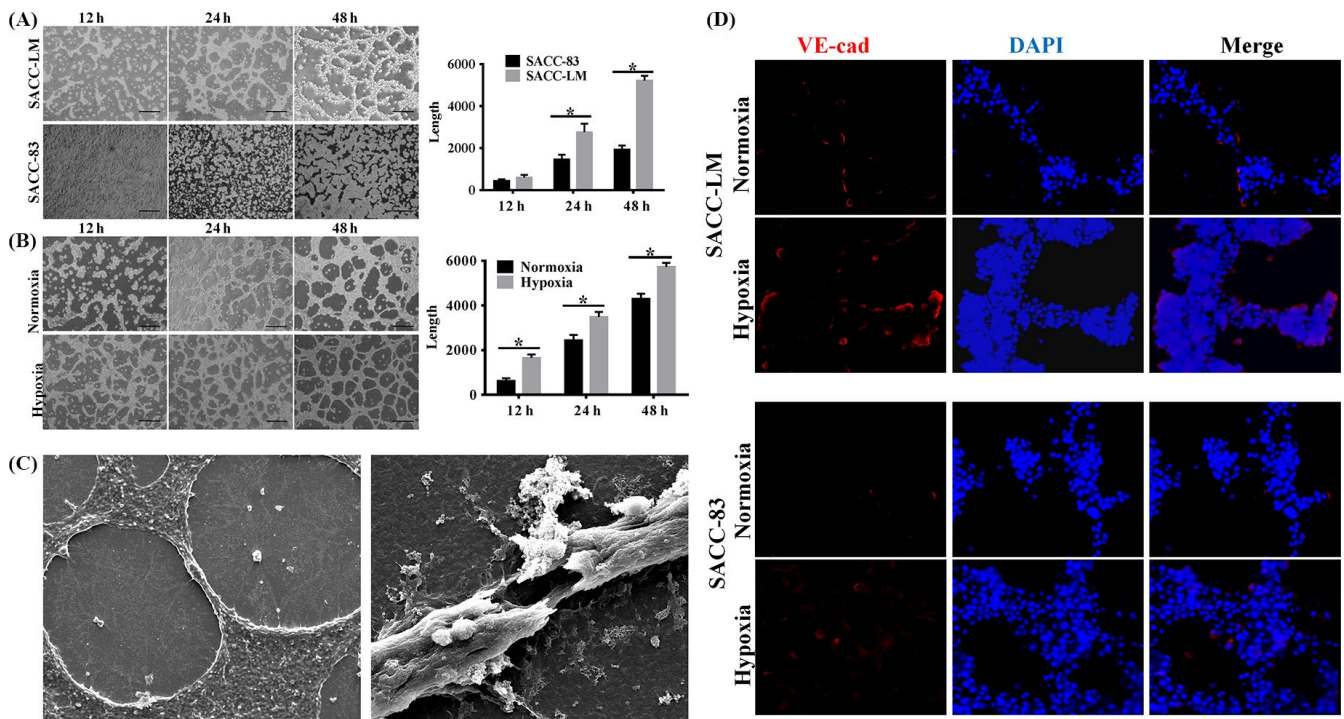


FIGURE 2 Effect of hypoxia on VM formation in SACC cell lines. A, Tube-like structure formation on Matrigel in SACC-LM and SACC-83 cells under normoxia. The SACC-LM showed a stronger ability of VM formation. For quantitative analysis, six nonoverlapping fields were selected from each culture well and the experiment was performed in quadruplicate ($*P < 0.05$). B, Hypoxia promoted the VM formation of SACC cells. For quantitative analysis, six nonoverlapping fields were selected from each culture well and the experiment was performed in quadruplicate. ($*P < 0.05$). C, Scanning electron microscopy was performed to show the tubular profiles were hollow and lined by flattened cancer cells after 7 days on the three-dimensional cultures. The panel on the left was representative image of cross section of tubular structure. The panel on the right was representative image of vertical section. D, The immunofluorescence staining showed that hypoxia promoted VE-cadherin of SACC cells

SACC-LM cells. Then, we further detected the relationship between hypoxia and EMT and found that SACC cells exhibited a significant up-regulation of mesenchymal markers, N-cadherin and Vimentin (Figure 1C), meanwhile dramatically down-regulation of E-cadherin (Figure 1D) by immunofluorescence. Real-time PCR analyses also revealed that the mRNA expression of E-cadherin decreased, as well as N-cadherin and Vimentin mRNAs increased in SACC-83 and SACC-LM cells under hypoxia (Figure 1E). Besides, the expression of EMT associated transcription factors, Twist1, Snail, and Slug1 also up-regulated under hypoxia in SACC cells (Figure S1A). These suggested that hypoxia promoted migration and invasion, and EMT of SACC cells.

3.2 | Hypoxia promoted VM formation in SACC cells

Then, we plated SACC cell lines, SACC-83 and SACC-LM, on the surface of Matrigel to establish the 3D culture model, and assessed the ability of VM formation under hypoxia during 48 hours. Our data showed that SACC-LM cells with high metastatic potential exhibited the formation of channel-like structures after 12 hours incubation on matrigel in normoxia or hypoxia group. After 48 hours, we observed interconnected loops and networks in SACC-LM cells in both normoxia and hypoxia groups. In contrast, there were less tubular or

sinusoidal channels in poor metastatic SACC-83 cells (Figure 2A). For the two cell lines, quantification of the length of channel-like structures showed that there was a significant increase after 48 hours incubation in hypoxia in comparison with normoxia condition ($P < 0.05$, Figure 2B). To further define the structure of the tubular networks, scanning electron microscopy was performed on the three-dimensional cultures. We found that tubular profiles were hollow and lined by flattened cancer cells after 7 days (Figure 2C). Furthermore, immunofluorescence staining revealed that the expression of VE-cadherin, marker of VM, enhanced in SACC-LM under hypoxia, compared to normoxia. However, there was no statistical difference between the normoxia and hypoxia group in SACC-83 cells (Figure 2D). Besides, the mRNA levels of VEGFR1 and VEGFR2, markers of VM, remarkably enhanced under hypoxia (Figure S1B). These results suggested that the vital role of hypoxic condition in the formation of vasculogenic-like networks and metastatic potential was positive correlation with the ability of VM formation in SACC in vitro.

3.3 | VEGFA was crucial for hypoxia-induced VM of SACC cells in vitro

As we known, VEGFA plays a key role in tumour-associated angiogenesis, but its role in vasculogenic mimicry remains unclear. In

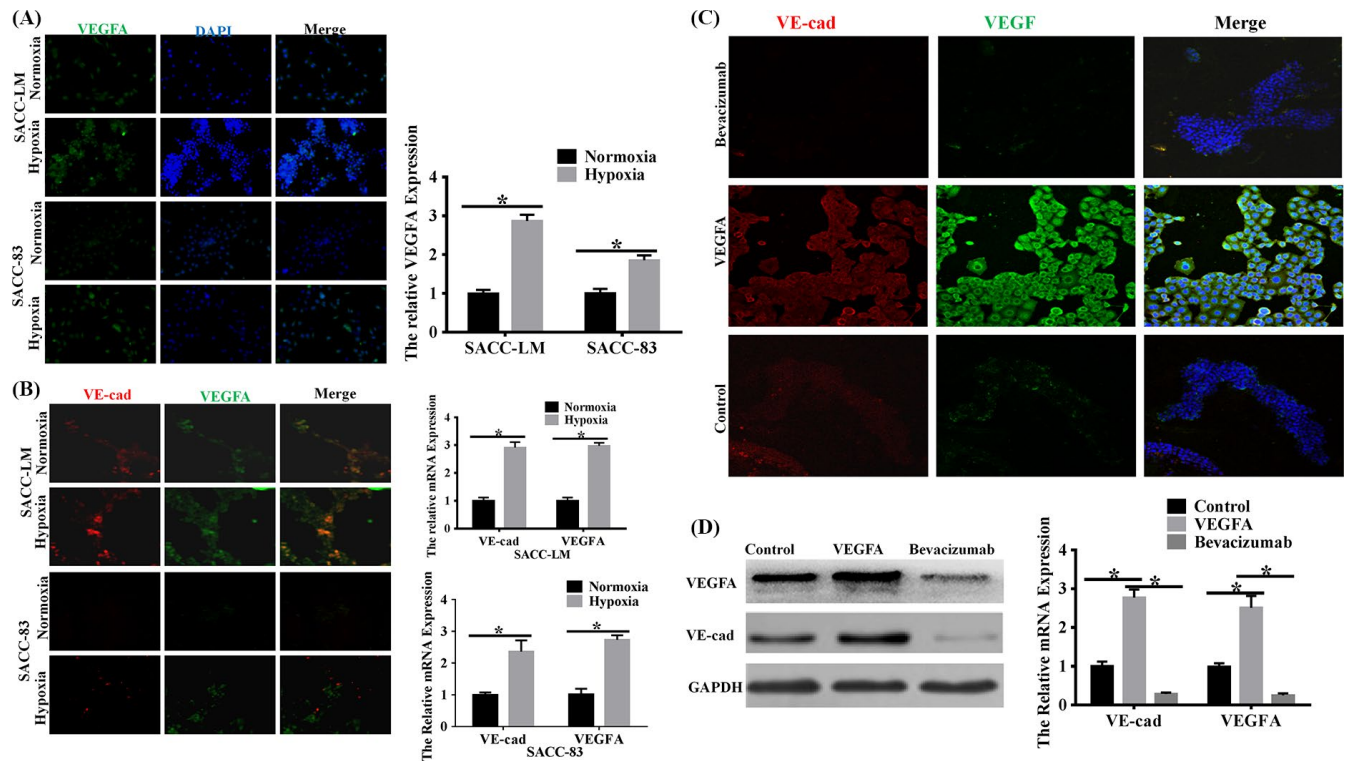


FIGURE 3 VEGFA was involved in VM formation of SACC-LM and SACC-83 cells in vitro. A, Immunofluorescence staining and RT-PCR assessed the effect of hypoxia on VEGFA protein and mRNA expression in SACC cell lines, respectively. The data showed that hypoxia enhanced the level of VEGFA of SACC cells in 2D culture in both protein and mRNA levels (magnification, $\times 100$; bars, $100 \mu\text{m}$, $*P < 0.05$). B, VEGFA expression in SACC-LM and SACC-83 cells was assessed by immunofluorescence staining and RT-PCR. The data showed that VEGFA was overexpression accompanied by high expression of VE-cadherin under hypoxia (magnification, $\times 100$; $*P < 0.05$). C, CLSM (magnification, $\times 200$) was performed to assess the role of VEGFA on VE-cadherin of SACC-LM cells. The data showed that VEGFA enhanced the level of VE-cadherin while bevacizumab suppressed its expression. D, Western blot was performed to assess the role of VEGFA on VE-cadherin of SACC-LM cells. The data showed that VEGFA enhanced the level of VE-cadherin while bevacizumab suppressed its expression. E, RT-PCR ($*P < 0.05$) was performed to assess the role of VEGFA on VE-cadherin of SACC-LM cells. The data showed that VEGFA enhanced the level of VE-cadherin while bevacizumab suppressed its expression

order to answer this question, we first compared VEGFA expression in SACC-83 and SACC-LM cells by immunofluorescence and RT-PCR. Our results demonstrated that VEGFA expression was elevated in SACC-LM owning higher VM-forming potential compared to SACC-83 cells owning poor VM-forming potential, especially under hypoxia condition (Figure 3A). Then, tube formation assay was conducted by seeding cells on Matrigel and we assessed the level of VEGFA in VM-forming SACC cells. We found that the expression of VEGFA remarkably increased in tube-forming cells under hypoxic niche, especially in SACC-LM (Figure 3B). It hinted that VEGFA was associated with VM formation in hypoxia. So we next treated SACC-LM cells with exogenous VEGFA or bevacizumab under hypoxia. After 6 hour incubation on matrigel, compared to the control group or VEGFA-inhibition group, the SACC-LM cells treated with VEGFA showed morphological changes and tendency to form VM-structures. After 48 hours, both the VEGFA-stimulated group and control group formed typical tube-like structures, while there were just a few such structures in VEGFA-inhibited group (Figure 3C). Subsequently, we investigated the effect of VEGFA on the level of VE-cadherin in hypoxic microenvironment. Compared to the control group, exogenous VEGFA could enhance the mRNA and

protein levels of VE-cadherin under hypoxia assessed by RT-PCR and Western blot, respectively. Contrarily, bevacizumab declined the expression of VE-cadherin (Figure 3D). The expression of VE-cadherin was in accordance with the level of VEGFA. These data indicated a possible role of VEGFA in regulating the hypoxia-induced tube formation capability of SACC in vitro.

3.4 | VEGFA resulted in hypoxia-induced VM formation by inducing EMT in SACC

For epithelial tumour cells, the capability of mimicking endothelial functions played an important role in VM formation.²² Thus, we speculated that VEGFA contributed to hypoxia-mediated VM-forming though inducing EMT. Our results showed that overexpressed VEGFA in SACC-LM led to remarkably increased N-cadherin expression while E-cadherin was almost undetectable in the hypoxia-stimulated tube structures in both mRNA and protein levels after 48 hours seeded on Matrigel. The inhibition of VEGFA was associated with a marked decrease in N-cadherin and unchanged level in E-cadherin (Figure 4A,B). It was documented that EMT endowed epithelial cancer cells with the self-renewal capacity.²³ And our group previously

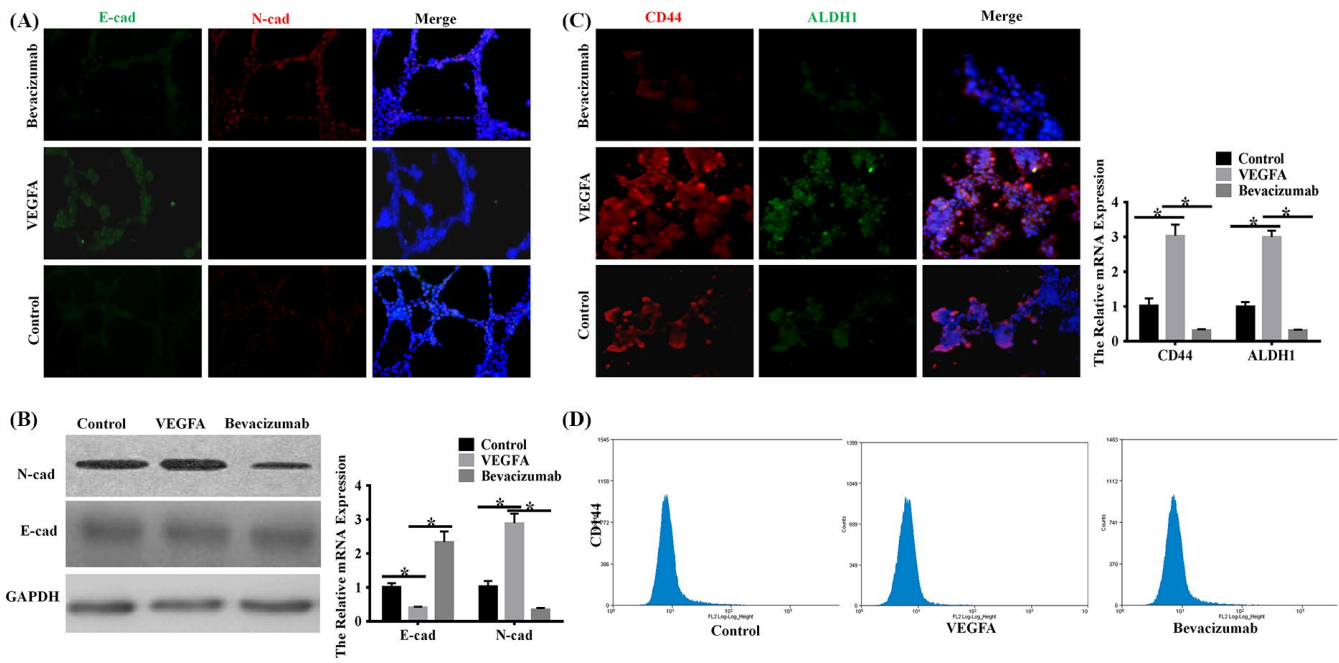


FIGURE 4 Exogenous VEGFA promoted EMT and stemness of SACC cells in vitro. A, Immunofluorescence staining (magnification, $\times 100$) was performed to assess the role of VEGFA on EMT of SACC-LM cells. The data showed that VEGFA enhanced the level of N-cadherin and inhibition the expression of E-cadherin while bevacizumab resulted in reverse changes. B, Western blot and RT-PCR ($*P < 0.05$) were performed to assess the role of VEGFA on EMT of SACC-LM cells. The data showed that VEGFA enhanced the level of N-cadherin and inhibition the expression of E-cadherin while bevacizumab resulted in reverse changes. C, Immunofluorescence staining (magnification, $\times 100$; bars, $100 \mu\text{m}$) and RT-PCR ($*P < 0.05$) were performed to assess the role of VEGFA on stemness of SACC-LM cells. The data showed that VEGFA enhanced the levels of CD44 and ALDH1 while bevacizumab resulted in reverse changes. D, Flow cytometry showed that the expression of CD144 had no difference among three groups

proved that CD133⁺, the stemness marker, was positively associated with VM formation in SACC specimens.²¹ Therefore, we inferred that VEGFA also contributed to the acquisition of stem cell phenotype in SACC cells. Immunofluorescence staining revealed that compared to the control group, SACC-LM treated with exogenous VEGFA showed the increase of stemness marker-CD44 and ALDH1 expression in VM-forming cells. On the contrary, bevacizumab led to a significant decrease in CD44 and ALDH1 expression of tube-forming cells (Figure 4C). However, the flow cytometry showed that the expression of CD144, another stemness marker, had no difference among the three groups (Figure 4C). We assessed the sphere formation of SACC-LM under the stimulation of exogenous VEGFA or bevacizumab. And we observed that the exogenous VEGFA heightened the sphere-forming capacity while bevacizumab inhibited the tumoursphere formation (Figure S1C). Collectively, these experiments suggested that VEGFA promoted hypoxia-induced VM formation, which may be mediated by the EMT process and cancer stem cells (CSCs) in SACC cells in vitro.

3.5 | Presence of VM in SACC tissues correlated with high expressions of VEGFA and HIF-1 α

The presence of VM was authenticated by the presence of PAS-positive loops and/or contained red blood cells that were negative for the endothelial cell marker CD31, while the endothelial vascular

channels were positive for CD31 staining (Figure 5A). As shown in Table 1, 25 tissue samples from 95 cases of SACC (26.3%) were VM positive. In addition, there was a significant association between the presence of VM and the clinic stage ($P = 0.006$) and distant metastases ($P = 0.000$), but there was no association between VM and patients' age, gender, position and pathological subtypes ($P > 0.05$). As shown in Figure 5B, high levels of expression of VEGFA was present in 47 of the 95 cases (49.47%) and in 18 of the 25 VM-positive samples (72.0%) but in only 29 of the 70 VM-negative samples (41.43%). VEGFA staining was mainly cytoplasmic. Statistically, there was a significant correlation between high expression of VEGFA and presence of VM ($r = 0.412$, $P = 0.000$) (Figure 5B). The positive staining of HIF-1 α was located in the cytoplasm and the nuclei. Statistically, there was a significant correlation between high expression of HIF-1 α and presence of VM ($r = 0.457$, $P = 0.000$; Figure 5C). Taken together, the results show a positive association of VM and VEGFA or HIF-1 α in SACC.

4 | DISCUSSION

Hypoxia, a common characteristic of solid tumours, has been reported to activate migration, invasion and VM formation in several tumour models including melanoma,²³ oral squamous cell carcinoma²⁴ and glioma.²⁵ Here, we found that hypoxia accelerated VM

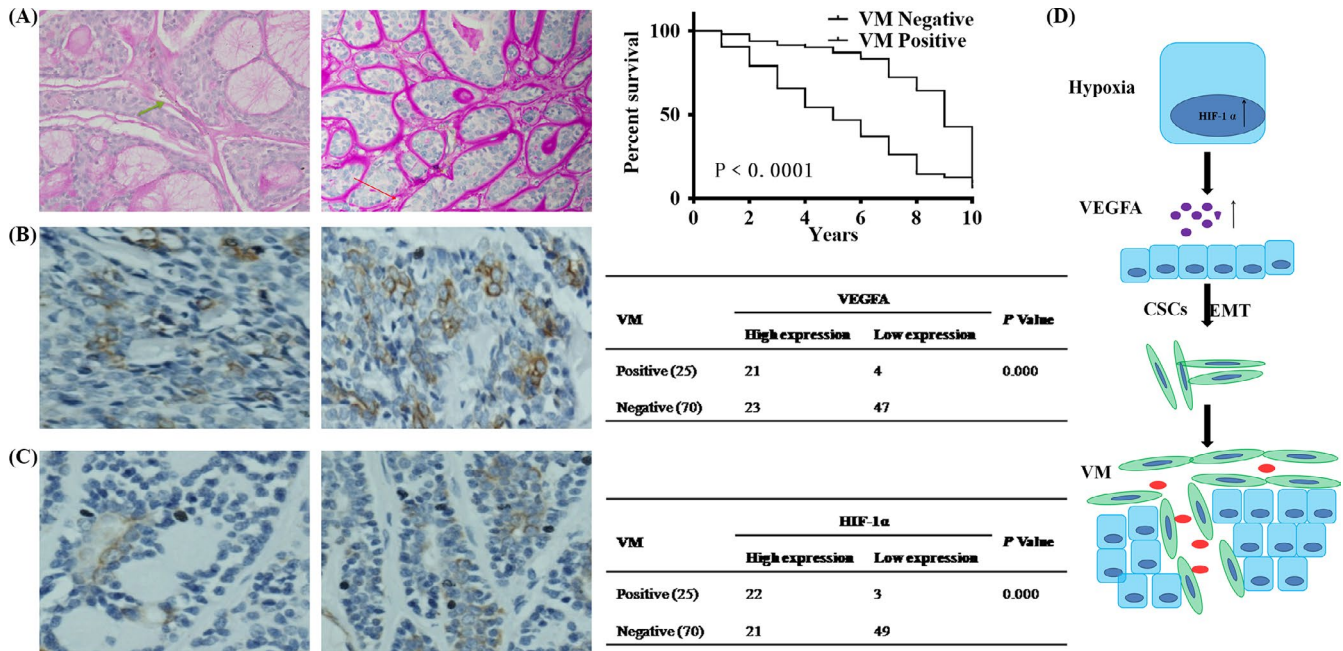


FIGURE 5 VM formation correlated with VEGFA and HIF-1 α expression in SACC tissues. A, CD31/PAS double staining was utilized to access the presence of VM. The panel on the left showed endothelial cell-dependent blood vessels which were CD31⁺PAS⁻ channels (green arrow). The panel on the right showed VM which was CD31⁺PAS⁺ (red arrow) (magnification, $\times 100$). B, VEGFA in SACC showed mainly cytoplasmic staining (magnification, $\times 100$). Different expression levels of VEGFA in VM-positive and VM-negative tumours from the two distinct SACC patients, and the evaluation of the relationship between VEGFA expression and VM formation in SACC tissues using χ^2 tests. C, HIF-1 α in SACC showed mainly cytoplasmic and nuclear staining (magnification, $\times 100$). Different expression levels of HIF-1 α in VM-positive and VM-negative tumours from the two distinct SACC patients, and the evaluation of the relationship between HIF-1 α expression and VM formation in SACC tissues using χ^2 tests. D, Schematic representation of the role of VEGFA in VM formation of SACC

formation of SACC and VEGFA was a critical downstream molecule that mediated the hypoxia-controlled SACC VM in vitro. And we identified that VEGFA regulated the cell plasticity and stemness to promote VM formation of SACC cells. In addition, the high expression of HIF-1 α and VEGFA obviously associated with the VM density in SACC samples. Thus, the current study linked VEGFA and consequential activation of EMT and stemness with VM formation in SACC and indicated the potential of VEGFA to act as therapeutic targets in SACC.

Here, we found that the migration and invasion abilities of SACC cells under hypoxic condition were stronger than under normoxia in vitro, and hypoxia induced EMT of SACC cells. In line with our study, hypoxic microenvironment could accelerate the migration and invasion of both MDA-MB-231 cells and MCF-7 cells.²⁶ Kim et al²⁷ illustrated that hypoxic condition augmented the aggressive phenotypes including mobility and invasiveness of human malignant mesothelioma cells in vitro. Lin et al²⁸ found that hypoxia induced the EMT and facilitated cancer dissemination in non-small cell lung cancer cells. Then, the data of the 3D culture conformed that hypoxic condition significantly promoted the formation of tube-like structures and the expression of VE-cadherin compared to normoxia in SACC cells, and the presence of VM was positively related to the high expression of HIF-1 α . In agreement with our results, Du et al¹⁶ found that hypoxia increased VM formation of ovarian cancer cell lines SKOV3 and OVCAR3 in vitro. Wang et al¹⁴ demonstrated that the high

expression of HIF-1 α was positive correlation with VM in 201 HCC sample tissues. Salinas-Vera et al¹³ observed a dramatic increase in VM-related structures when triple negative breast cancer cell lines MDA-MB-231 and Hs-578T cells were grown after 12 hour hypoxic incubation on Matrigel. These indicated that hypoxia promoted the aggressiveness of SACC cells.

A number of previous studies have demonstrated that hypoxia closely associated with angiogenesis via VEGFA^{29,30}; however, it is unclear whether VEGFA has equally important significance in hypoxia-induced VM in SACC. Our results showed that VEGFA was remarkably increased in SACC cells under hypoxia condition. Exogenous VEGFA strengthened the capability of forming vessel-like structures and VE-cadherin expression, while bevacizumab obviously restrained VM formation and VE-cadherin expression. Moreover, the high level of VEGFA showed a significant correlation with the VM in SACC tissues. The data were supported by the report of Vartanian et al,³¹ who showed that VEGFA was essential for the initiation of melanoma cells into capillary-like structure in vitro. The knockdown of VEGFR1 completely prevented Matrigel-induced VM formation. Hence, VEGFA/VEGFR1 pathway was considered to contribute to the formation of VM in melanoma. Azad et al³² confirmed that VEGF/VEGFR promoted VM in MCF10 cells via Hippo pathway. These highlighted the role of VEGFA in promoting hypoxia-mediated VM in SACC. However, Xu et al³³ found that short-term anti-VEGFA treatment induced increase VM and metastasis in SKOV3^{LUC+}

TABLE 1 Clinicopathological features of SACC patients and their association with VM expression

Clinicopathological features	n	VM		P value
		Positive (n = 25)	Negative (n = 70)	
Age				
<45	38	9	29	0.635
≥45	57	16	41	
Gender				
Male	42	15	27	0.640
Female	53	10	43	
Site				
Major salivary gland	70	16	54	0.200
Minor salivary gland	25	9	16	
Clinic stage				
I/II	45	9	36	0.006
III/IV	50	19	31	
Histological subtype				
Tubular/cribriform	58	39	19	0.196
Solid	37	20	17	
Distant metastasis				
Yes	35	30	5	0.000
No	60	28	32	

tumour-bearing mice. Schnegg et al³⁴ found that tumour xenografts originated from sensitive to VEGFA inhibition underwent an adaptation *via* HIF-1 expression and an increase in CD144⁺ VM, while tumour xenografts of cell populations resistant to this inhibition did not exhibit these features compared to the control counterparts. Thus, VEGFA may perform different roles in the VM in the different tumour cell types and much should be done.

EMT, the reversible dedifferentiation process of polarized epithelial cells, has been shown to play an important role in acquiring endothelial-like properties to form vessel-like structures in epithelial cancers.³⁵ Meng et al³⁶ found that Hsp90 β enhanced the VE-cadherin promoter activity by interacting with EMT-related transcription factor Twist1 in hepatocellular carcinoma. Similarly, the high level of ZEB1, another EMT-related transcription factor, was strongly associated with the presence of VM in 96 prostate cancer samples ($P < 0.05$).³⁷ On the other hand, evidence confirmed that VEGFA stimulation of normal epithelial cells and differentiated carcinoma cells could induce an EMT. VEGFA could stimulate EMT of pancreatic neuroendocrine tumour cells *in vitro*.³⁸ In breast cancer, VEGFA led to EMT by up-regulating SOX2 expression *in vivo* and *in vitro*.³⁹ VEGFA could sustain EMT in sonic hedgehog medulloblastoma stem cells *via* Nrp2.⁴⁰ Hence, we proposed a hypothesis that VEGFA may accelerate hypoxia-induced VM by affecting EMT in SACC. In order to verify this, we examined the role of VEGFA in hypoxia-controlled VM formation in SACC. The data showed that exogenous VEGFA enhanced the expression of N-cadherin and sharply suppressed the expression of E-cadherin in channel-like structures. In the contrary, inhibition of VEGFA made N-cadherin down-regulate accompanied by unchanged E-cadherin level. These results strongly suggested

that VEGFA-induced EMT may a critical step in hypoxia-caused VM in SACC. Furthermore, EMT is considered to be sufficient to endow and maintain cancer cells with stemness. There are remarkable similarities between cancer stem cells (CSCs) and cancer cells with mesenchymal phenotype, both of which are highly invasive, resistant against common anticancer treatment and thought to cause metastatic growth. And the two phenotypes are reversible and can be interchanged *via* EMT or CSC phenotype interconversion.^{41,42} A growing body of evidence suggests that CSCs are also involved in regulating VM formation.⁴³ Hence, we assessed the effect of VEGFA on cancer cells stemness and found that overexpression of VEGFA accelerated stemness marker CD44 and ALDH1 expression in VM-forming SACC cells under hypoxia, while suppression of VEGFA reduced CD44 and ALDH1 expression. Similarly, Jang et al⁴⁴ found that VEGFA up-regulated Bmi1, tumourspheres and ALDH1 activity in primary human ovarian cancer cell lines *via* VEGFR2-dependent Src activation.⁴⁴ Ramezani et al⁴⁵ demonstrated that human glioblastoma stem-like cells promoted themselves proliferation by secreting the VEGFA in an autocrine manner. Therefore, we inferred that VEGFA may affect VM by endowing SACC cells stemness.

In addition, we detected PAS⁺/CD31⁻ vessel-like structure contained red blood cells in 25 of 95 SACC samples and the data showed that the VM positively correlated with advanced clinic stage and distance metastasis of SACC patients. Wang et al⁴⁶ showed that VM was detected in a total of 25 (27.2%) of 92 prostate cancer patients whose presence was positive correlation with advanced TNM stage ($P = 0.001$), and the presence of lymph node ($P = 0.001$) as well as distant metastases ($P = 0.025$). Williamson et al⁴⁷ pointed out that higher levels of VM were associated with worse 3-year survival in

41 limited-stage small cell lung cancer patients' biopsies ($P < 0.025$). You et al⁴⁸ demonstrated that VM was existent in 29/127 (22.8%) primary gastric cancer cases, and the presence of VM was associated with tumour size, differentiation, depth of tumour invasion, stage and lymph node metastases. The data confirmed that VM might be a poor prognosis marker of human carcinoma.

Taken together, in present study, we confirmed that hypoxia accelerated the VM of SACC cells, and VEGFA was a critical downstream molecule that mediated the hypoxia-controlled EMT inducing VM in SACC. In human SACC tissues, the presence of VM was positive correlation with the advanced clinic stage and distance metastasis, as well as the levels of VEGFA and HIF-1 α in SACC tissue. These indicated that hypoxia may serve as an inducer of VM in SACC by targeting VEGFA-mediated EMT, which provided a new sight in the search the therapeutic target of SACC.

ACKNOWLEDGMENTS

The present study was supported by National Natural Science Foundation of China grants (grant nos. 81672672, 81772891, 81572650 and 81502357), the Fundamental Research Funds for the Central Universities (2017), Natural Science Foundation of Zhejiang Province (grant no. Q142114001), Zhoushan Science and Technology Bureau Project (grant no. 2014C3106), and by Sichuan Province Science and Technology Bureau Project (2017JY0024).

CONFLICT OF INTEREST

The authors confirm that there are no conflicts of interest.

AUTHOR CONTRIBUTION

Study design: YLT, XHL; Data Collection: HFW, SSW, MZ, LLD, KW, XLG; Data analysis: MXC, XHY, XP, MZ, JBW; Manuscript preparation: JSW, XY, YJT, YC.

ORCID

Sha-sha Wang  <https://orcid.org/0000-0002-1181-1672>

REFERENCES

- Tian Z, Li L, Wang L, Hu Y, Li J. Salivary gland neoplasms in oral and maxillofacial regions: a 23-year retrospective study of 6982 cases in an eastern Chinese population. *Int J Oral Maxillofac Surg*. 2010;39:235-242.
- Wang Y, Zhang CY, Xia RH, et al. The MYB/miR-130a/NDRG2 axis modulates tumor proliferation and metastatic potential in salivary adenoid cystic carcinoma. *Cell Death Dis*. 2018;9:917.
- Zhang J, Peng B, Chen X. Expressions of nuclear factor kappaB, inducible nitric oxide synthase, and vascular endothelial growth factor in adenoid cystic carcinoma of salivary glands: correlations with the angiogenesis and clinical outcome. *Clin Cancer Res*. 2005;11:7334-7343.
- Yao X, Wang Y, Duan Y, et al. IGFBP2 promotes salivary adenoid cystic carcinoma metastasis by activating the NF- κ B/ZEB1 signaling pathway. *Cancer Lett*. 2018;432:38-46.
- Weng LX, Wang GH, Yao H, Yu MF, Lin J. Epigallocatechin gallate inhibits the growth of salivary adenoid cystic carcinoma cells via the EGFR/Erk signal transduction pathway and the mitochondria apoptosis pathway. *Neoplasma*. 2017;64:563-570.
- Adams A, Warner K, Nör JE. Salivary gland cancer stem cells. *Oral Oncol*. 2013;49:845-853.
- Maniotis AJ, Folberg R, Hess A, et al. Vascular channel formation by human melanoma cells in vivo and in vitro: vasculogenic mimicry. *Am J Pathol*. 1999;155:739-752.
- Zhang S, Fu Z, Wei J, Guo J, Liu M, Du K. Peroxiredoxin 2 is involved in vasculogenic mimicry formation by targeting VEGFR2 activation in colorectal cancer. *Med Oncol*. 2015;32:414.
- Tu DG, Yu Y, Lee CH, et al. Hinokitiol inhibits vasculogenic mimicry activity of breast cancer stem/progenitor cells through proteasome-mediated degradation of epidermal growth factor receptor. *Oncol Lett*. 2016;11:2934-2940.
- Ruffini F, Graziani G, Levati L, Tentori L, D'Atri S, Lacial PM. Cilengitide downmodulates invasiveness and vasculogenic mimicry of neuropilin 1 expressing melanoma cells through the inhibition of α v β 5 integrin. *Int J Cancer*. 2015;136:E545-558.
- Wang W, Lin P, Sun B, et al. Epithelial-mesenchymal transition regulated by EphA2 contributes to vasculogenic mimicry formation of head and neck squamous cell carcinoma. *Biomed Res Int*. 2014;2014:803914.
- Bai J, Yeh S, Qiu X, et al. TR4 nuclear receptor promotes clear cell renal cell carcinoma (ccRCC) vasculogenic mimicry (VM) formation and metastasis via altering the miR490-3p/vimentin signals. *Oncogene*. 2018;37:5901-5912.
- Salinas-Vera YM, Marchat LA, García-Vázquez R, et al. Cooperative multi-targeting of signaling networks by angiomiR-204 inhibits vasculogenic mimicry in breast cancer cells. *Cancer Lett*. 2018;432:17-27.
- Wang M, Zhao X, Zhu D, et al. HIF-1 α promoted vasculogenic mimicry formation in hepatocellular carcinoma through LOXL2 up-regulation in hypoxic tumor microenvironment. *J Exp Clin Cancer Res*. 2017;36:60.
- Wang Y, Sun H, Zhang D, et al. TP53INP1 inhibits hypoxia-induced vasculogenic mimicry formation via the ROS/snail signalling axis in breast cancer. *J Cell Mol Med*. 2018;22:3475-3488.
- Du J, Sun B, Zhao X, et al. Hypoxia promotes vasculogenic mimicry formation by inducing epithelial-mesenchymal transition in ovarian carcinoma. *Gynecol Oncol*. 2014;133:575-583.
- Li W, Zong SQ, Shi Q, Li HJ, Xu J, Hou FG. Hypoxia-induced vasculogenic mimicry formation in human colorectal cancer cells: involvement of HIF-1 α , Claudin-4, and E-cadherin and Vimentin. *Sci Rep*. 2016;6:37534.
- Ahluwalia A, Tarnawski AS. Critical role of hypoxia sensor HIF-1 α in VEGF gene activation. Implications for angiogenesis and tissue injury healing. *Curr Med Chem*. 2012;19:90-97.
- Duan L, Ye L, Zhuang L, et al. VEGFC/VEGFR3 axis mediates TGF β 1-induced epithelial-to-mesenchymal transition in non-small cell lung cancer cells. *PLoS ONE*. 2018;13:e0200452.
- Liu K, Sun B, Zhao X, et al. Hypoxia promotes vasculogenic mimicry formation by the Twist1-Bmi1 connection in hepatocellular carcinoma. *Int J Mol Med*. 2015;36:783-791.
- Wang SS, Gao XL, Liu X, et al. CD133+ cancer stem-like cells promote migration and invasion of salivary adenoid cystic carcinoma by inducing vasculogenic mimicry formation. *Oncotarget*. 2016;7:29051-29062.
- Li C, Zhu M, Lou X, et al. Transcriptional factor OCT4 promotes esophageal cancer metastasis by inducing epithelial-mesenchymal

- transition through VEGF-C/VEGFR-3 signaling pathway. *Oncotarget*. 2017;8:71933-71945.
23. Li W, Zhou Y. LRIG1 acts as a critical regulator of melanoma cell invasion, migration and vasculogenic mimicry upon hypoxia by regulating EGFR/ERK-triggered EMT. *Biosci Rep*. 2019;39:BSR20181165.
 24. Liu R, Wang HL, Deng MJ, et al. Melatonin inhibits reactive oxygen species-driven proliferation, epithelial-mesenchymal transition, and vasculogenic mimicry in oral cancer. *Oxid Med Cell Longev*. 2018;2018:3510970.
 25. Duan S. Silencing the autophagy-specific gene Beclin-1 contributes to attenuated hypoxia-induced vasculogenic mimicry formation in glioma. *Cancer Biomark*. 2018;21:565-574.
 26. Li S, Zhang Q, Zhou L, et al. Inhibitory effects of compound DMBT on hypoxia-induced vasculogenic mimicry in human breast cancer. *Biomed Pharmacother*. 2017;96:982-992.
 27. Kim MC, Hwang SH, Kim NY, et al. Hypoxia promotes acquisition of aggressive phenotypes in human malignant mesothelioma. *BMC Cancer*. 2018;18:819.
 28. Lin SC, Chung CH, Chung CH, et al. OCT4B mediates hypoxia-induced cancer dissemination. *Oncogene*. 2018;38:1093-1105.
 29. Xu S, Zhang J, Xue H, et al. MicroRNA-584-3p reduces the vasculogenic mimicry of human glioma cells by regulating hypoxia-induced ROCK1 dependent stress fiber formation. *Neoplasma*. 2017;64:13-21.
 30. Tang NN, Zhu H, Zhang HJ, et al. HIF-1 α induces VE-cadherin expression and modulates vasculogenic mimicry in esophageal carcinoma cells. *World J Gastroenterol*. 2014;20:17894-17904.
 31. Vartanian A, Stepanova E, Grigorieva I, Solomko E, Baryshnikov A, Lichinitser M. VEGFR1 and PKC α signaling control melanoma vasculogenic mimicry in a VEGFR2 kinase-independent manner. *Melanoma Res*. 2011;21:91-98.
 32. Azad T, Janse van Rensburg HJ, Lightbody ED, et al. A LATS biosensor screen identifies VEGFR as a regulator of the Hippo pathway in angiogenesis. *Nat Commun*. 2018;9:1061.
 33. Xu Y, Li Q, Li XY, Yang QY, Xu WW, Liu GL. Short-term anti-vascular endothelial growth factor treatment elicits vasculogenic mimicry formation of tumors to accelerate metastasis. *J Exp Clin Cancer Res*. 2012;31:16.
 34. Schnegg CI, Yang MH, Ghosh SK, Hsu MY. Induction of vasculogenic mimicry overrides VEGF-A silencing and enriches stem-like cancer cells in melanoma. *Cancer Res*. 2015;75:1682-1690.
 35. Adhim Z, Matsuoka T, Bito T, et al. In vitro and in vivo inhibitory effect of three Cox-2 inhibitors and epithelial-to-mesenchymal transition in human bladder cancer cell lines. *Br J Cancer*. 2011;105(3):393-402.
 36. Meng J, Chen S, Lei YY, et al. Hsp90 β promotes aggressive vasculogenic mimicry via epithelial-mesenchymal transition in hepatocellular carcinoma. *Oncogene*. 2018;38:228-243.
 37. Wang H, Huang B, Li BM, et al. ZEB1-mediated vasculogenic mimicry formation associates with epithelial-mesenchymal transition and cancer stem cell phenotypes in prostate cancer. *J Cell Mol Med*. 2018;22:3768-3781.
 38. Chiang KC, Yeh CN, Pang JS, et al. 1 α ,25(OH)₂D₃ analog, MART-10, inhibits neuroendocrine tumor cell metastasis after VEGF-A stimulation. *Anticancer Res*. 2017;37:6215-6221.
 39. Kim M, Jang K, Miller P, et al. VEGFA links self-renewal and metastasis by inducing Sox2 to repress miR-452, driving Slug. *Oncogene*. 2017;36:5199-5211.
 40. Besharat ZM, Sabato C, Po A, et al. Low expression of miR-466f-3p sustains epithelial to mesenchymal transition in sonic hedgehog medulloblastoma stem cells through Vegfa-Nrp2 signaling pathway. *Front Pharmacol*. 2018;9:1281.
 41. Mani SA, Guo W, Liao MJ, et al. The epithelial-mesenchymal transition generates cells with properties of stem cells. *Cell*. 2008;133:704-715.
 42. Chen C, Okita Y, Watanabe Y, et al. Glycoprotein nmb is exposed on the surface of dormant breast cancer cells and induces stem cell-like properties. *Cancer Res*. 2018;78:6424-6435.
 43. Fan YL, Zheng M, Tang YL, Liang XH. A new perspective of vasculogenic mimicry: EMT and cancer stem cells (Review). *Oncol Lett*. 2013;6:1174-1180.
 44. Jang K, Kim M, Gilbert CA, Simpkins F, Ince TA, Slingerland JM. VEGFA activates an epigenetic pathway upregulating ovarian cancer-initiating cells. *EMBO Mol Med*. 2017;9:304-318.
 45. Ramezani S, Vousooghi N, Kapourchali FR, et al. Rolipram potentiates bevacizumab-induced cell death in human glioblastoma stem-like cells. *Life Sci*. 2017;173:11-19.
 46. Wang H, Lin H, Pan J, et al. Vasculogenic mimicry in prostate cancer: the roles of EphA2 and PI3K. *J Cancer*. 2016;7:1114-1124.
 47. Williamson SC, Metcalf RL, Trapani F, et al. Vasculogenic mimicry in small cell lung cancer. *Nat Commun*. 2016;7:13322.
 48. You X, Wang Y, Wu J, et al. Prognostic significance of galectin-1 and vasculogenic mimicry in patients with gastric cancer. *Onco Targets Ther*. 2018;11:3237-3244.

SUPPORTING INFORMATION

Additional supporting information may be found online in the Supporting Information section at the end of the article.

How to cite this article: Wang H-F, Wang S-S, Zheng M, et al. Hypoxia promotes vasculogenic mimicry formation by vascular endothelial growth factor A mediating epithelial-mesenchymal transition in salivary adenoid cystic carcinoma. *Cell Prolif*. 2019;52:e12600. <https://doi.org/10.1111/cpr.12600>